Tuning the Viscoelasticity of

Hydrogen-Bonded Polymeric Materials

through Solvent Composition

Lele Mathis⁺, Yaoyao Chen⁺, and Kenneth R. Shull*

Department of Materials Science and Engineering, Northwestern University, Evanston, IL,

60208, USA

E-mail: k-shull@northwestern.edu

⁺These authors contributed equally to this work.

Abstract

The interactions between polymer molecules in solution are strongly affected by the way that

the constituent polymers interact with the solvent. In this work, we use a mixed solvent system

(dimethyl sulfoxide and ethylene glycol) to tailor the strength of the hydrogen bonding interactions

between partially quaternized poly (4-vinyl pyridine) [QVP] and poly (methacrylic acid) [PMAA].

The charge introduced by the quaternization reaction enables homogeneous solutions to be formed

over a large concentration range, even in the presence of attractive hydrogen bonding interactions

between the proton-donating PMAA and the proton-accepting QVP. The viscoelastic properties of

equimolar QVP/PMAA solutions are superposed onto master curves that are well-described by a

fractional Maxwell liquid model. This model provides a means for quantifying the dependence of the

relaxation times on the solvent composition. These relaxation times increase by a factor of 1000 as the

hydrogen bonding interactions are strengthened by a decrease in the DMSO content of the solvent,

1

within a composition regime where the solutions remain homogeneous. A much stronger effect is obtained when the ethylene glycol is replaced by water.

Introduction

Polymeric materials bonded by weak interactions, such as hydrogen bonding, ¹ electrostatic interactions, ^{2–5} host-guest inclusion, ^{6,7} *etc.*, find applications in a variety of fields including drug delivery, functional coatings, and underwater adhesion. ^{8–10} The weak nature of these interactions allows them to reform under mild conditions, enabling a range of useful material responses. ^{8,11–15} The phase behavior and dynamic response of these systems are influenced by the strength of the intermolecular bonding interactions in a non-trivial way. One important consideration in the application of these materials is their processiability, which can be affected by altering the nature of the bonding within material to obtain a more liquid-like or solid-like response. ¹⁶ For example, salt concentration has been widely used to control electrostatic interactions between oppositely charged polyelectrolytes, producing moldable materials at high salt concentrations that transform to stiffer materials after dialysis. ^{17–19} A general understanding of the interplay between viscoelastic properties, material composition and environmental parameters (temperature, ionic strength of the surrounding medium, *etc.*) is essential when designing processing routes and application areas for functional materials made from associating polymer solutions.

The focus of the work reported here is on polymer solutions and gels where the dynamics are controlled by intermolecular hydrogen bonding interactions, using solvent composition to control the hydrogen bonding strength. We use poly(methacrylic acid) (PMAA) as the proton donor and poly(4-vinylpyridine) (P4VP) as the proton acceptor. This system, and closely related systems involving poly(2-vinyl pyridine) or poly(acrylic acid), have been widely investigated for a range of applications and as model systems. $^{20-28}$ In aqueous media, these materials are weak polyelectrolytes, with pK_a values in the accessible range (4.7 for P4VP and 5.5 for PMAA). 29 Under conditions where one or both of the polymers are charged, electrostatic interactions affect the assembly and the solubility of the complexes in the solvent, 30,31 but are not necessarily the most important factors in determining the rheological response of the material at a fixed overall polymer concentration. 32

In our previous work, we demonstrated that the transient network built up by partially quaternized poly (4- vinyl pyridine) (QVP) and PMAA could be used to strengthen and toughen ABA triblock copolymer hydrogels.³² The interactions between QVP and PMAA, and the resultant toughness of the gels, are found to be sensitive to the details of the solvent. We also found that the role of un-quaternized groups

(P4VP) is more significant than that of charged groups in terms of interacting with PMAA. To develop an understanding of the role of solvent in the QVP-PMAA system, where the dynamics are determined by hydrogen bonding interactions between proton-donating and proton-accepting groups, we performed a more systematic study of the effects of solvent composition on the complexes formed between PMAA and QVP. We considered a range of solvents, but we focused primarily on mixtures of either water or ethylene glycol with DMSO, a hydrogen bond acceptor that is well-known for its ability to disrupt hydrogen bonding. 33–38

Materials and Methods

Materials

Poly (4-vinyl pyridine) (P4VP, molecular weight, 200,000 g/mol), and poly (methacrylic acid) (PMAA), were purchased from Scientific Polymer Products Incorporation and used without further purification. Figure 3(a) shows the structures of P4VP, quaternized poly (4-vinyl pyridine), and PMAA. Organic solvents, methanol (MeOH), ethanol (EtOH), ethylene glycol (EG), dimethyl sulfoxide (DMSO), dimethyl formamide (DMF), and N-methyl-2-pyrrolidone (NMP) were purchased from Sigma-Aldrich, and were also used as received. Physical properties of these solvents are listed in Table 1, and all of these solvents could be utilized to dissolve homopolymers, P4VP and PMAA. Quaternization of P4VP was achieved by adding a certain amount of ethyl bromide (Sigma-Aldrich) into P4VP solution to reach the expected charge ratio, which was confirmed by ¹H-NMR, in a Bruker Advance III 500 MHz system (¹H-NMR spectra shown in Supporting information). We refer to this partially quaternized polymer as QVPxx, where xx is the mole percent quaternization. QVP and PMAA (at a molar ratio of 1:1 based on the concentrations of the acrylic acid and pyridyl units) were dissolved in the solvent mixture of interest to make samples for rheological testing, with a total polymer weight fraction of 9.1 wt.% in each case.

Characterization

Solubility tests: The solubility of single component systems (PMAA, P4VP, QVPxx) was tested by making solutions at overall polymer concentrations of 2 wt.%. Clear polymer solutions were obtained

in most solutions of individual polymers in different solvents, except for high charge ratio QVP in NMP and DMF, shown in Table 2. The polymer blend systems (QVP-PMAA or P4VP-PMAA) in Table 2 correspond to equimolar mixtures (based on the concentrations of pyridyl and methacrylic acid groups) at a total polymer weight fraction of 9.1 *wt.*%. Either white precipitates or homogeneous clear solutions/gels were obtained after mixing two types of polymers, with results shown in Table 2.

Rheological experiments: Rheological behaviors of QVPxx-PMAA solutions were probed by an Anton Paar MCR 302 rheometer using a stainless steel cone—plate geometry (50 mm in diameter, 2° angle). All experiments were conducted at 25 °C. Frequency sweeps were performed from 0.1 rad/s to 100 rad/s in the linear viscoelastic regime (strain amplitudes less than 5%). We also conducted steady state shear tests on these samples, in the shear rate range, $\dot{\gamma}$ =0.01-100 s⁻¹. The zero shear viscosity (η_o) of each specimen was obtained from the low shear rate region ($\dot{\gamma}$ <10 s⁻¹), where the viscosity value was independent of shear rate.

Fractional Maxwell liquid model fitting: The model we utilized to simulate the frequency responses of our materials is a fractional Maxwell liquid model, consisting of a spring-pot, and a dash-pot (in Figure 1). ³⁹ The dash-pot represents the viscous part of the material, with the viscosity of η_o , dominating the long term relaxation at low frequency regime. At higher frequencies, the spring-pot plays a more important role, determining the phase angle at short time scales. ^{40,41}

The spring-pot element is a power-law element, with a constant phase angle across the frequency range. The complex shear modulus of a spring-pot is expressed as:

$$G^* = G^S(i\omega/\omega_o)^\beta \tag{1}$$

where ω_o is reference frequency and G^S is the magnitude of the complex modulus at this reference frequency. The exponent, β ($0 \le \beta \le 1$) is the most important parameter in this expression, and is directly related to the phase angle, δ ($\beta = \delta/90^\circ$). Note that $\beta=0$ corresponds to a pure solid with $\delta=0^\circ$, and $\beta=1$ represents a Newtonian liquid with $\delta=90^\circ$.

In the fractional Maxwell liquid model, a liquid element with an exponent of 1 is placed in series with a springpot characterized by an exponent of β . The connection of these two elements gives the responses

of a typical fractional Maxwell liquid:

$$\frac{G^*}{G^S} = \frac{(i\omega\tau)^{\beta}}{1 + (i\omega\tau)^{\beta - 1}} \tag{2}$$

Here τ is the inverse of the characteristic frequency at which the power law response transitions from 1 to β , and G^S is closely related to the modulus of the material at this transition point. By adjusting three parameters, τ , β , and G^S , the full spectrum can be simulated. The zero shear viscosity is obtained directly from G^S and τ :

$$\eta_o = G^S \tau \tag{3}$$

As an example, Figure 1 shows the response of the system for $\beta = 0.3$, which is very close to the value obtained from our experiments. One advantage of using this model is the simplicity of the fitting process. Only three parameters need to be used, while traditional viscoelastic liquid models involve the fitting of multiple Maxwell elements. ⁴⁰ More detailed explanations of our implementation of the fractional Maxwell liquid model can be found elsewhere. ³⁹

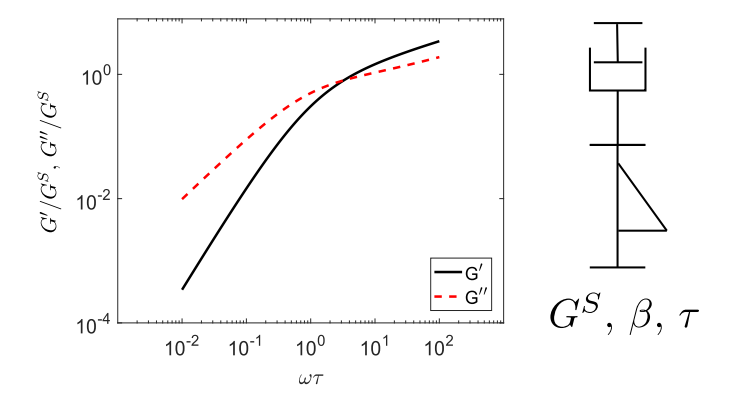


Figure 1: A spectrum predicted by the factional Maxwell liquid model, with $\beta = 0.30$.

Results and Discussion

Phase Diagram

In this work we study the role of solvents in determining the viscoelastic properties of polyelectrolyte complexes, beginning with the solvents listed in Table 1. The solubility of the different polymers and polymer mixtures are listed in Table 2. While PMAA and P4VP are soluble in a wide range of solvents, mixtures of these polymers generally form precipitates due to the strong hydrogen bonding interactions between these two polymers, with PMAA acting as a proton donor and P4VP acting as a proton accepter. 42–44 The exception is DMSO, which is an effective proton accepter, reducing the net interaction between the polymers so that a homogeneous solution is maintained. Proton accepting polymers, including, for example, poly (vinyl pyrrolidone) (PVP), poly (vinyl alcohol) (PVA), poly (ethylene oxide) (PEO), or QVP in our case, remain flowable in the presence of PMAA in DMSO. 42 Regardless of the changes in charge fraction in QVP, DMSO provides an ideal environment for dissolving and processing polymer mixtures for useful applications. 1,9

Table 1: Properties of different solvents in this work. *Dielectric constants of organic solvents come from Ref. ⁴⁵

Solvents	*arepsilon	Nature
Water	78.5	Protic solvent
Ethanol (EtOH)	22.4	Protic solvent
Methanol (MeOH)	32.6	Protic solvent
Ethylene glycol (EG)	37.7	Protic solvent
Dimethyl sulfoxide (DMSO)	46.6	Aprotic solvent
N,N-dimethylformamide (DMF)	36.7	Aprotic solvent
N-methyl-2-pyrrolidone (NMP)	32.2	Aprotic solvent

In our previous work, water was added as a co-solvent to DMSO in order to strengthen the hydrogen bonding interactions between QVP and PMAA, tuning the rheological and fracture properties of the QVP-PMAA complexes.³² However, to obtain homogeneous samples, the degree of charge within the QVP was restricted to values from 5% to 25%, and the water content within the solvent was restricted to values less than 40%. A better solvent mixture is needed to broaden the range of materials that can be used. Ethylene glycol (EG) is a particularly attractive co-solvent choice because of the wide range of solution compositions and charge ratios over which single phase QVP-PMAA complexes can be obtained.

Table 2: Solubility of polymers and polymer mixtures in different solvents. Clear solutions were obtained for the polymer/solvent combinations for which an X is shown in the table. The total polymer weight fraction for testing mixed polymer solubility was 9.1 wt.% ^a The solubility information of P4VP in water was taken from reference ⁴⁶.

Solvents	$H_2O (pH=7)$	EtOH	MeOH	EG	DMSO	DMF	NMP
PMAA	X	X	X	X	X	X	X
P4VP	X (pH<5) ^a	X	X	X	X	X	X
QVP20	X	X	X	X	X	X	X
QVP30	X	X	X	X	X	X	X
QVP50	X	X	X	X	X	X	
QVP70	X	X	X	X	X		
P4VP-PMAA					X		
QVP30-PMAA					X		
QVP50-PMAA				X	X		
QVP70-PMAA				X	X		

Mixtures of ethylene glycol and DMSO are ideally suited as a model system for tailoring the strength of hydrogen bonding interactions in QVP-PMAA for this reason, and are investigated in the most detail in the work presented here.

The dependencies of solubility on both solvent composition and quaternization degree for equimolar blends of QVP and PMAA in DMSO-EG solvent mixtures are shown in Figure 2. Higher degrees of charge enhance the solubility of the complexes. When the degree of charge on the QVP polymer is larger than 50%, the solutions are soluble for all DMSO-EG solvent compositions. QVP-PMAA mixtures made with QVP10 (a 10% degree of charge) are soluble for ethylene glycol contents of 50 *wt*.% or less, and mixtures made with QVP20 (a 20% degree of charge) are soluble for ethylene glycol contents of 70 *wt*.% or less. This behavior is determined by the combination of hydrogen bonding, electrostatic interactions, and counterion entropy. The importance of hydrogen bonding in this system is consistent with previous investigations of hydrogen bonding in similar polymer complexes formed by P4VP, where a mild shifts in the the characteristic adsorption peaks are observed in FT-IR experiments. ^{21,22}

Rheological Characterization

The decreased solubility of the polymers as the ethylene glycol content in the solvent increases can be attributed to an increase in strength of the net attractive interactions between the QVP and PMAA polymers. This enhanced interaction also increases the viscosity, as illustrated in Figure 3. Increasing the EG

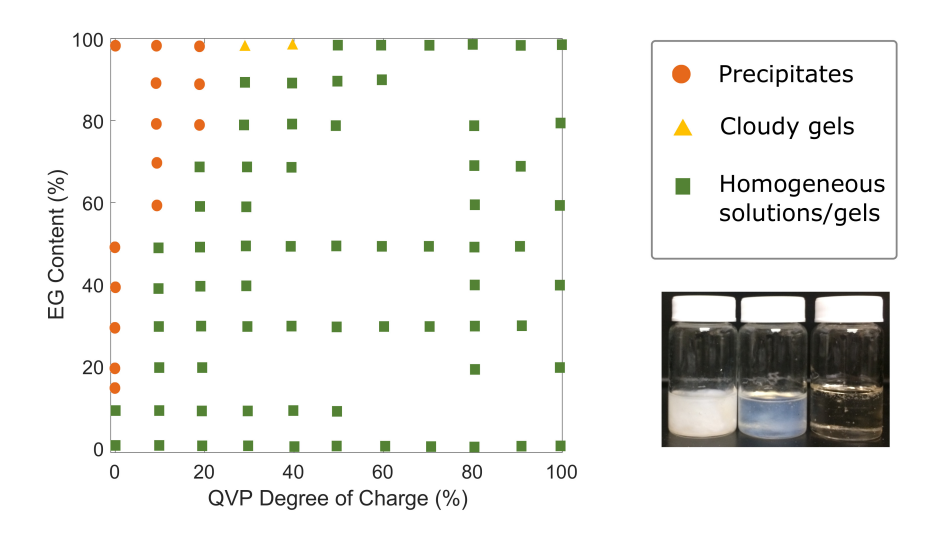


Figure 2: Phase behavior of QVPxx-PMAA system in DMSO-EG mixed solvents.

content to 60 wt.% in mixed solvents increases the viscosity by a factor of \sim 300 for the QVP20-PMAA system, and by a factor of \sim 1000 for the QVP10-PMAA system. Complexes formed between PMAA and the fully quaternized system (QVP100) show a specific viscosity that is only weakly dependent on the solvent content, indicating that observed viscosity enhancement can be attributed to interactions between methacrylic acid and unquaternized 4-vinylpyridine groups.

The viscosity enhancement in mixed solvent conditions suggests that there exist strong attractive associations between polymers, leading to a strong dependence of viscosity on polymer concentration as well. ⁴⁷ Thus, a slight change in polymer concentration in our experiments would induce a more significant difference in viscosity value, resulting in the mild scattering in the experimental results in 20% and 30% EG samples in QVP20-PMAA system, shown in Figure 3(b). In pure DMSO, a general trend of decreasing in viscosity is observed as charge ratio increases. Dou *et al.* ²⁷ suggested that the introduction of charges to poly (vinyl pyridine) has a significant impact on the correlation of polymer chains, which possibly contributes to the observed viscosity change for different charge ratios. It also needs to be mentioned that although DMSO is a good hydrogen bonding disruper for QVP-PMAA, the intermolecular bonding between QVP and PMAA might still play a role. As charge ratio increases, the density of these bondings decreases, giving lower viscosity values.

Figure 4 and Figure 5 give a more quantitative description of the rheology of these solutions. The increase of ethylene glycol content results in a higher magnitude of the complex modulus, and a lower phase

angle, as illustrated in Figure 4. As shown in Figure 5(a), superposition of the frequency-dependent storage and loss moduli at different solvent compositions is obtained by applying horizontal solvent shift factors, a_S , to the data. These shift factors are referenced to the pure DMSO solvents (ethylene glycol content=0), for which a_s is defined to be equal to 1. The composition dependencies of these shift factors are shown in Figure 5(b). We also show the solvent shift factors obtained for QVP10-PMAA and QVP30-PMAA systems in Figure 5(b). The reduced charge density in the QVP10 polymer enhances the ability for intermolecular hydrogen bonds to form, giving larger values of a_S (and therefore of the zero-shear viscosity, which is proportional to a_S , shown in Supporting Information) than those are observed for the QVP20-PMAA system. However, in QVP30-PMAA, there is an overall decrease in the value of a_S compared with QVP20-PMAA, due to the lower probability of complexation through hydrogen bonding.

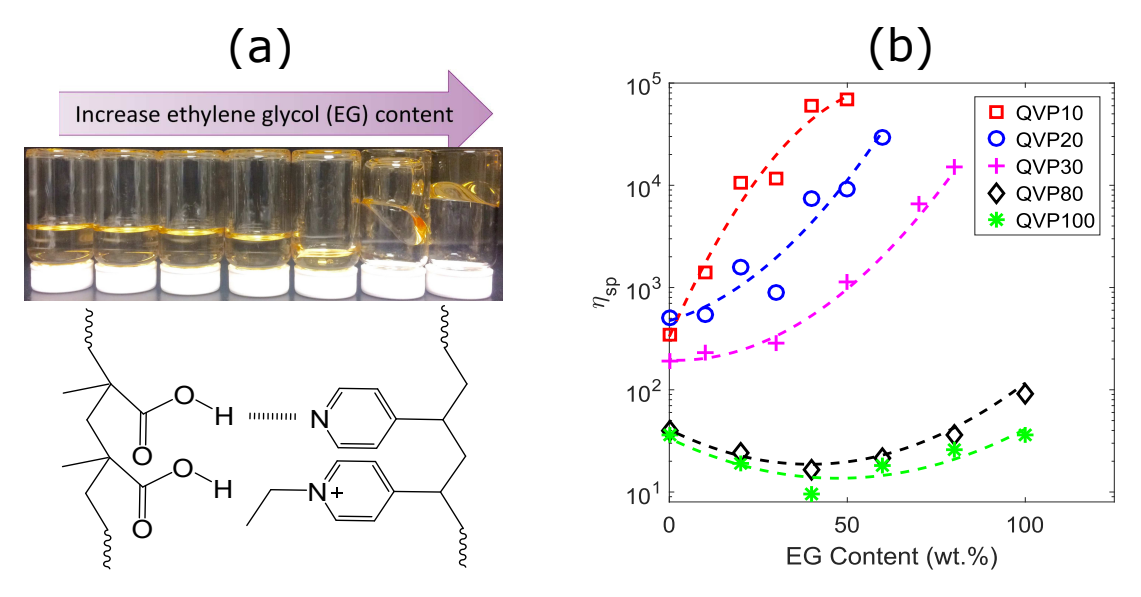


Figure 3: (a) Images of QVP20-PMAA blends dissolved in different DMSO-EG mixtures. The enhanced viscosity as the ethylene glycol content is increased from 0 to 60 wt.% in 10 wt. % increments from left to right is illustrated. A schematic representation of hyrogen bonding between the PMAA and QVP polymers is also shown. (b) Effect of DMSO-EG solvent composition on the specific viscosity of equimolar mixtures of QVP10, QVP20, QVP30, QVP80, or QVP100, and PMAA, at a total polymer concentration of 9.1 wt. %. $\eta_{sp} = (\eta_o - \eta_{solvent})/\eta_{solvent}$. The viscosities of mixed solvents are based on literature. ⁴⁸ The legends in (b) denote mixtures of two types of polymers.

Fractional Maxwell Liquid Models for DMSO-EG and DMSO-Water Systems

In order to understand the role of different solvents in determining rheological properties of these model hydrogen bonding systems, it is useful to compare the behavior DMSO-EG and DMSO-water mixed

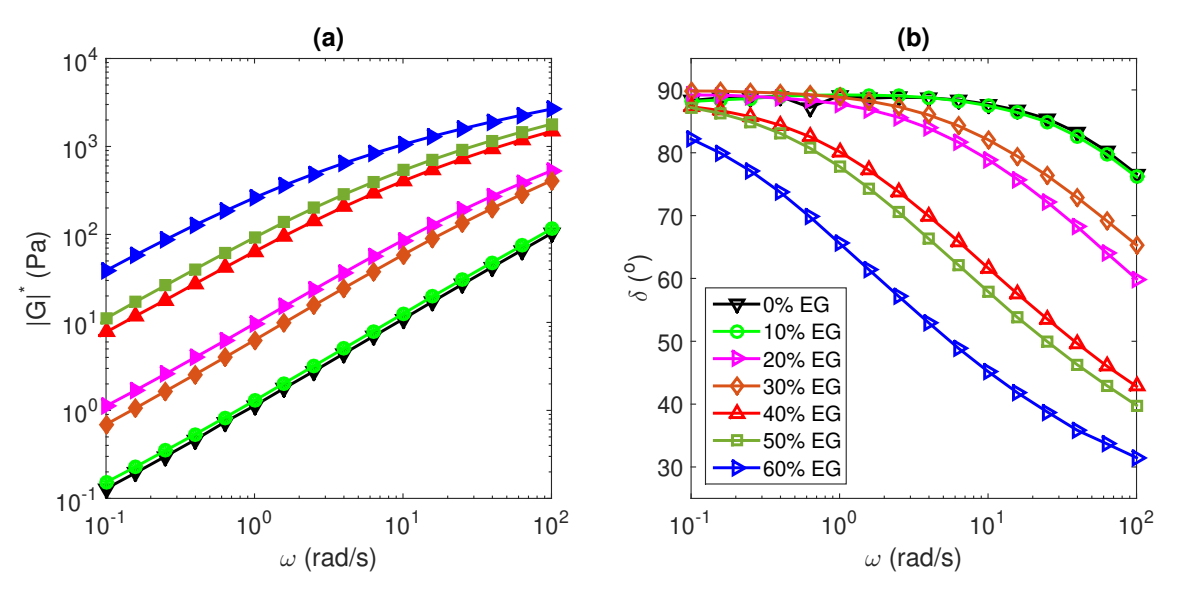


Figure 4: Rheology of QVP20-PMAA in DMSO-EG solution. (a) $|G|^*$ as a function of shear frequency; (b) frequency dependence of phase angle $(\delta = \arctan(G''/G'))$.

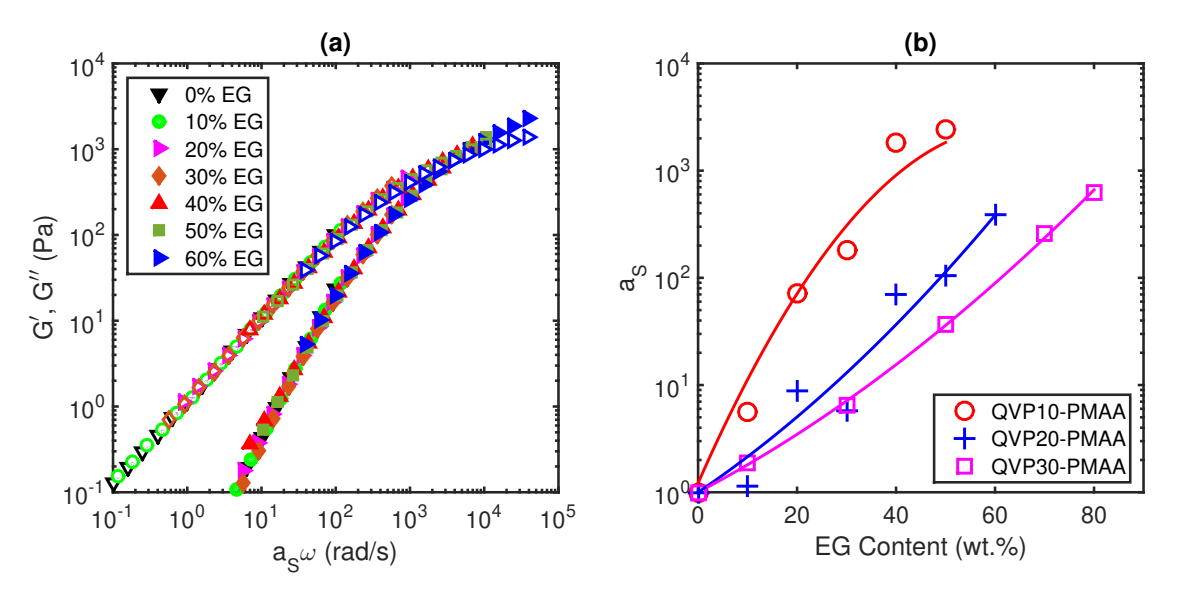


Figure 5: (a) Master curves for G' (filled symbols) and G'' (open symbols) for the QVP20-PMAA system for DMSO-EG solvent mixtures; (b) solvent shift factors used to generate the master curves in QVP10-PMAA, QVP20-PMAA, and QVP30-PMAA systems.

solvent systems. This comparison is made in Figure 6 for the equimolar mixtures of QVP20 and PMAA at the same total polymer concentration of 9.1 *wt*. % that is used in the rest of this work. Rheological master curves are shown in parts (a) and (b) of this figure for the DMSO-EG and DMSO-water solvent systems, respectively. In DMSO intermolecular hydrogen bonding is disrupted. Although both water and ethylene glycol are able to strengthen the QVP-PMAA intermolecular interactions, water is much more efficient than ethylene glycol at promoting hydrogen bond formation between the methacrylic acid and vinyl pyridine units of the constituent polymers, with the viscosity increasing much more rapidly with the addition of water than it does with the addition of ethylene glycol.

Table 3: Fractional Maxwell model fitting parameters for QVP20-PMAA.

Solvent	G^{S} (Pa)	β	EG/Water content (wt%)	a_S	τ (s)	η_o (Pa·s)
DMSO-EG	1000	0.31	0	1	0.0010	1.0
			10	1.1	0.0011	1.7
			20	8.8	0.0088	9.0
			30	5.7	0.0057	7.5
			40	69	0.069	80
			50	105	0.11	115
			60	386	0.39	408
DMSO-Water	800	0.31	0	1	0.0010	0.8
			5	1.7	0.0017	1.3
			10	3.6	0.0036	2.5
			15	13	0.013	8.8
			20	50	0.05	32
			25	220	0.22	148
			30	1500	1.5	1020

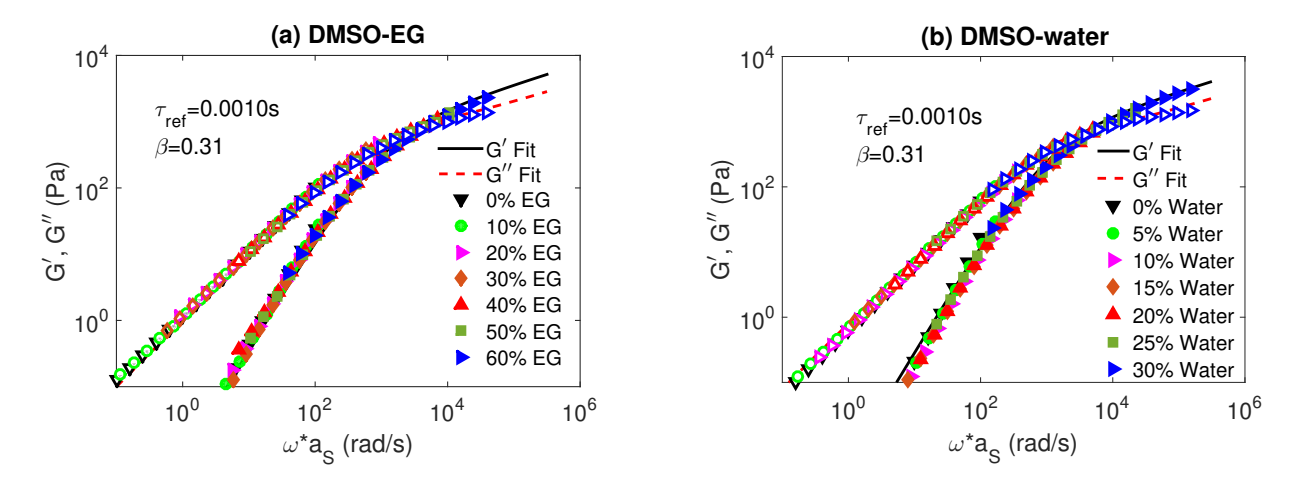


Figure 6: Behavior of QVP20-PMAA in DMSO-EG (a) and DMSO-water (b) mixed solvents.

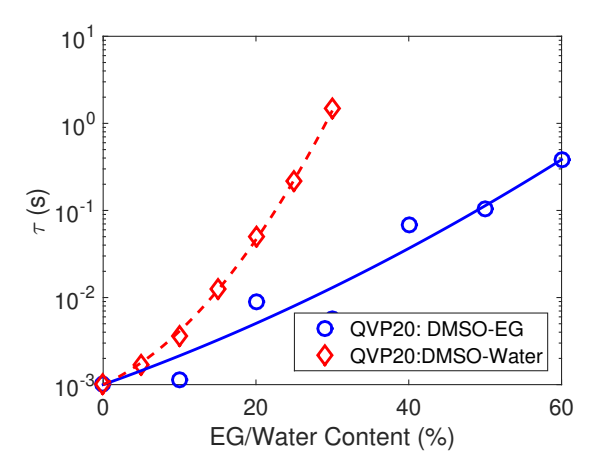


Figure 7: Relaxation times for the QVP20-PMAA system for the DMSO-water and DMSO-EG mixed solvent systems.

To quantify the behavior of QVP20-PMAA in different solvent systems, these master curves are fitted to fractional Maxwell liquid models (Eq. 2), with fitting parameters listed in Table 3. We obtain $\beta \approx 0.31$ for the DMSO-EG, and DMSO-water systems. The relaxation times, τ , in Table 3 are proportional to both η_0 (Eq. 2) and a_S , so any of these three quantities can be taken as a measure of the effect of the solvent composition on the dynamics of the solutions. In Figure 7 we plot τ as a function of solvent composition for the QVP20-PMAA system. These are the characteristic time-scales where the material transitions from liquid-like behavior with $|G^*| \propto \omega$ to a gel-like behavior where $|G^*| \propto \omega^{0.31}$. Use of the fractional Maxwell liquid model enables us to quantify changes in the solvent-dependent dynamics by specifying this single parameter.

It has been demonstrated that fractional Maxwell model is able to probe the viscoelastic properties of QVP-PMAA system by adjusting three parameters in this case. The choice of these parameters depends on the structures of the materials. Sadman *et al.* applied the same model to a series of fully quaternized poly (4-vinyl pyridine) - polystyrene sulfonate (QVP-PSS) coacervates, obtaining $\beta \approx 0.41$. Samp *et al.* fitted this model to tough hydrogels, and obtained β values between 0.05 and 0.15. Factors that influence viscoelasticity of the materials will lead to different fitting parameters. System, the nature of interactions that drive the complexation, mobility of polymer chains, molecular weights and concentration of polymers, are presumably to be factors that result in different viscoelastic properties, and fitting parameters. Exploring the correlation between rheological properties and the details of molecular structures in our polymers, for example, entanglements, is still of great interest for us,

and that will be our future work.

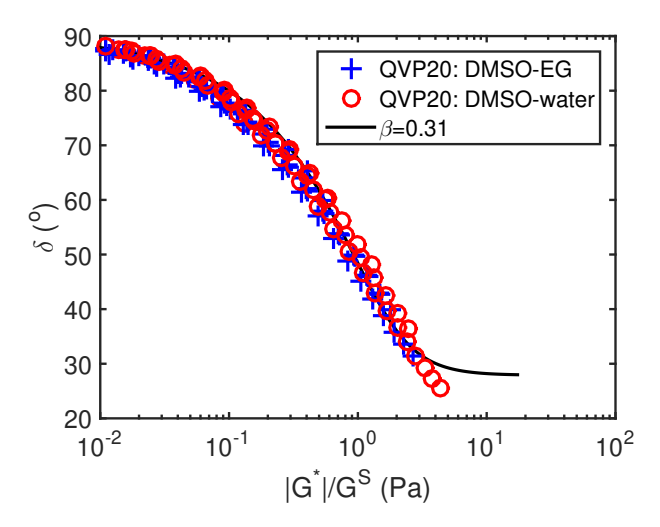


Figure 8: A van Gurp-Palmen plot showing phase angle as a function of the normalized magnitude of complex modulus of QVP20-PMAA systems both DMSO-EG and DMSO-water mixed solvents.

Universality of Mixed Solvent Effect

The overall picture emerging from this work is the nature of the solvents increases the relaxation times in the system by a solvent-dependent shift factor, a_S , but the shape of the relaxation time distribution is not affected. For this reason master-curves of similar shapes are obtained for different solvent mixtures. This point is further illustrated in Figure 8 where the viscoelastic phase angle is plotted as a function of normalized magnitude of the complex shear modulus for all of the data from parts (a) and (b) of Figure 6. In this plot, we also include the prediction of the fractional Maxwell liquid model, using $\beta = 0.31$. This type of plot, referred to as a van Gurp-Palmen plot, is normally used to generalize the responses of rubber materials under different temperatures and frequencies. $^{51-53}$ Collapse of the data onto a single curve indicates that the shape of the relaxation time distribution is not affected by the strength of hydrogen bonds that are responsible for the increased relaxation times in the system. During the addition of a different solvent (EG or water), only time scale that allows for the interaction relaxes is altered. Use of mixed solvents provides a facile tool for tuning the strength of interactions between polymers, leading to different viscoelastic properties and relaxation times; while the generalized viscoelastic responses of the system are dominated by structural features of the polymer complexes that are strongly affected by solvent composition.

One last point we want to address in Figure 8 is that the fractional Maxwell liquid model gives an accurate prediction in the more liquid-like regime where the complex modulus is relatively low and the phase angle is high. However, in the more solid-like regime at the highest frequencies, a discrepancy between the fractional Maxwell liquid model and the experimental data is observed. The model assumes a constant phase angle of $\beta * 90^{\circ}$ at high frequencies, but the experimental phase angle at the highest frequencies in our experiments decreases below this data. A more complete (and necessarily more complicated model) is needed in order to describe the data at the highest frequencies. Here we emphasize that fractional Maxwell liquid model, fully described by three independent parameters, gives an excellent description of the experimental data, greatly simplifying the comparison of related materials systems.

Conclusions

In conclusion, we have developed a system consisting of partially quaternized poly (4 vinyl pyridine) (QVP) and poly (methacrylic acid) (PMAA), and have studied the behavior of this system in mixed solvents of dimethyl sulfoxide (DMSO) and ethylene glycol (EG). The partial quaternization introduces a net repulsive interaction between polymer molecules in the system, decoupling the hydrogen bonding interactions that affect the rheological response of the system and the phase behavior. This strategy is used to quantify the effect of solvent composition on the hydrogen bonding interactions. Addition of either water or ethylene glycol increases hydrogen bond strength, with the addition of water increasing the relaxation times in the system more than the introduction of ethylene glycol, but with an enhancement of the relaxation times of up to three orders of magnitude in both cases. By using a simple fractional Maxwell liquid model, the viscoelastic properties of these materials could be simulated, providing a useful means for analyzing associating polymeric materials in general.

Acknowledgements

The authors acknowledge the funding support from NSF DMR Polymers Program (DMR-1410968 and DMR-1710491), the 3M Graduate Fellowship program, the REU program of the Northwestern University MRSEC (NSF grant DMR-1121262), and the Center for Hierarchical Materials Design (CHiMaD). This

work utilized the IMSERC facility at Northwestern University, which has received support from the Soft and Hybrid Nanotechnology Experimental (SHyNE) Resource (NSF NNCI-1542205), the State of Illinois and the International Institute for Nanotechnology. The authors also want to thank Kazi Sadman for his help in fitting fractional Maxwell models.

References

- (1) Ding, H.; Zhang, X. N.; Zheng, S. Y.; Song, Y.; Wu, Z. L.; Zheng, Q. Hydrogen bond reinforced poly(1-vinylimidazole- co -acrylic acid) hydrogels with high toughness, fast self-recovery, and dual pH-responsiveness. *Polymer* **2017**, *131*, 95–103, DOI: 10.1016/j.polymer.2017.09.044.
- (2) Fu, J.; Schlenoff, J. B. Driving Forces for Oppositely Charged Polyion Association in Aqueous Solutions: Enthalpic, Entropic, but Not Electrostatic. *Journal of the American Chemical Society* **2016**, *138*, 980–990, DOI: 10.1021/jacs.5b11878.
- (3) Wang, Q.; Schlenoff, J. B. The Polyelectrolyte Complex/Coacervate Continuum. *Macromolecules* **2014**, *47*, 3108–3116, DOI: 10.1021/ma500500q.
- (4) Zhang, P.; Zheng, P.-Y.; Zhao, F.-Y.; An, Q.-F.; Gao, C.-J. Preparation and pervaporation characteristics of novel ethanol permselective polyelectrolyte–surfactant complex membranes. *RSC Adv.* 2015, 5, 63545–63552, DOI: 10.1039/C5RA09308B.
- (5) Fu, J.; Fares, H. M.; Schlenoff, J. B. Ion-Pairing Strength in Polyelectrolyte Complexes. *Macro-molecules* **2017**, *50*, 1066–1074, DOI: 10.1021/acs.macromol.6b02445.
- (6) Takashima, Y.; Sawa, Y.; Iwaso, K.; Nakahata, M.; Yamaguchi, H.; Harada, A. Supramolecular Materials Cross-Linked by Host-Guest Inclusion Complexes: The Effect of Side Chain Molecules on Mechanical Properties. *Macromolecules* 2017, 50, 3254–3261, DOI: 10.1021/acs.macromol.7b00266.
- (7) Miao, T.; Fenn, S. L.; Charron, P. N.; Oldinski, R. A. Self-Healing and Thermoresponsive

- Dual-Cross-Linked Alginate Hydrogels Based on Supramolecular Inclusion Complexes. *Biomacro-molecules* **2015**, *16*, 3740–3750, DOI: 10.1021/acs.biomac.5b00940.
- (8) Heinzmann, C.; Weder, C.; de Espinosa, L. M. Supramolecular polymer adhesives: advanced materials inspired by nature. *Chem. Soc. Rev.* **2016**, *45*, 342–358, DOI: 10.1039/C5CS00477B.
- (9) Zhao, Q.; Lee, D. W.; Ahn, B. K.; Seo, S.; Kaufman, Y.; Israelachvili, J. N.; Waite, J. H. Underwater contact adhesion and microarchitecture in polyelectrolyte complexes actuated by solvent exchange. *Nature Materials* **2016**, *15*, 407–412, DOI: 10.1038/nmat4539.
- (10) Sadman, K.; Wang, Q.; Chen, S. H.; Delgado, D. E.; Shull, K. R. pH-Controlled Electrochemical Deposition of Polyelectrolyte Complex Films. *Langmuir* 2017, 33, 1834–1844, DOI: 10.1021/acs.langmuir.6b04491.
- (11) Liu, F.; Urban, M. W. Recent advances and challenges in designing stimuli-responsive polymers. *Progress in Polymer Science* **2010**, *35*, 3–23, DOI: 10.1016/j.progpolymsci.2009.10.002.
- (12) Holten-Andersen, N.; Harrington, M. J.; Birkedal, H.; Lee, B. P.; Messersmith, P. B.; Lee, K. Y. C.; Waite, J. H. pH-induced metal-ligand cross-links inspired by mussel yield self-healing polymer networks with near-covalent elastic moduli. *Proceedings of the National Academy of Sciences* 2011, 108, 2651–2655.
- (13) Henderson, K. J.; Zhou, T. C.; Otim, K. J.; Shull, K. R. Ionically Cross-Linked Triblock Copolymer Hydrogels with High Strength. *Macromolecules* **2010**, *43*, 6193–6201, DOI: 10.1021/ma100963m.
- (14) Wang, W.; Zhang, Y.; Liu, W. Bioinspired fabrication of high strength hydrogels from non-covalent interactions. *Progress in Polymer Science* **2017**, *71*, 1–25, DOI: 10.1016/j.progpolymsci.2017.04.001.
- (15) Creton, C. 50th Anniversary Perspective: Networks and Gels: Soft but Dynamic and Tough. *Macro-molecules* **2017**, *50*, 8297–8316, DOI: 10.1021/acs.macromol.7b01698.
- (16) Henderson, K. J.; Shull, K. R. Effects of Solvent Composition on the Assembly and Relaxation

- of Triblock Copolymer-Based Polyelectrolyte Gels. *Macromolecules* **2012**, *45*, 1631–1635, DOI: 10.1021/ma201607m.
- (17) Meng, X.; Perry, S. L.; Schiffman, J. D. Complex Coacervation: Chemically Stable Fibers Electrospun from Aqueous Polyelectrolyte Solutions. *ACS Macro Letters* **2017**, *6*, 505–511, DOI: 10.1021/acsmacrolett.7b00173.
- (18) Luo, F.; Sun, T. L.; Nakajima, T.; Kurokawa, T.; Ihsan, A. B.; Li, X.; Guo, H.; Gong, J. P. Free Reprocessability of Tough and Self-Healing Hydrogels Based on Polyion Complex. *ACS Macro Letters* **2015**, *4*, 961–964, DOI: 10.1021/acsmacrolett.5b00501.
- (19) Luo, F.; Sun, T. L.; Nakajima, T.; Kurokawa, T.; Zhao, Y.; Sato, K.; Ihsan, A. B.; Li, X.; Guo, H.; Gong, J. P. Oppositely Charged Polyelectrolytes Form Tough, Self-Healing, and Rebuildable Hydrogels. *Advanced Materials* **2015**, *27*, 2722–2727, DOI: 10.1002/adma.201500140.
- (20) Zhou, X.; Goh, S. H.; Lee, S. Y.; Tan, K. L. XPS and FTi. r. studies of interactions in poly (carboxylic acid)/poly (vinylpyridine) complexes. *Polymer* **1998**, *39*, 3631–3640.
- (21) ElMiloudi, K.; Benygzer, M.; Djadoun, S.; Sbirrazzuoli, N.; Geribaldi, S. FT-IR Spectroscopy and Hydrogen Bonding Interactions in Poly(styrene-co-methacrylic acid)/Poly(styrene-co-4-vinyl pyridine) Blends. *Macromolecular Symposia* **2005**, *230*, 39–50, DOI: 10.1002/masy.200551140.
- (22) Bennour, S.; Metref, F.; Djadoun, S. Hydrogen-bonding interactions between poly(styrene-comethacrylic acid) and poly(styrene-co-4-vinylpyridine). *Journal of Applied Polymer Science* **2005**, 98, 806–811, DOI: 10.1002/app.22088.
- (23) Jin, H.; An, Q.; Zhao, Q.; Qian, J.; Zhu, M. Pervaporation dehydration of ethanol by using polyelectrolyte complex membranes based on poly (N-ethyl-4-vinylpyridinium bromide) and sodium carboxymethyl cellulose. *Journal of Membrane Science* **2010**, *347*, 183–192, DOI: 10.1016/j.memsci.2009.10.023.
- (24) Warnant, J.; Marcotte, N.; Reboul, J.; Layrac, G.; Aqil, A.; Jerôme, C.; Lerner, D. A.; Gérardin, C. Physicochemical properties of pH-controlled polyion complex (PIC) micelles of poly(acrylic acid)-

- based double hydrophilic block copolymers and various polyamines. *Analytical and Bioanalytical Chemistry* **2012**, *403*, 1395–1404, DOI: 10.1007/s00216-012-5947-1.
- (25) Nguyen, V. T. A.; De Pauw-Gillet, M.-C.; Sandre, O.; Gauthier, M. Biocompatible Polyion Complex Micelles Synthesized from Arborescent Polymers. *Langmuir* **2016**, *32*, 13482–13492, DOI: 10.1021/acs.langmuir.6b03683.
- (26) Swift, T.; Seaton, C. C.; Rimmer, S. Poly(acrylic acid) Interpolymer Complexes. *Soft Matter* **2017**, *13*, 8736–8744, DOI: 10.1039/C7SM01787A.
- (27) Dou, S.; Colby, R. H. Charge density effects in salt-free polyelectrolyte solution rheology. *Journal of Polymer Science Part B: Polymer Physics* **2006**, *44*, 2001–2013, DOI: 10.1002/polb.20853.
- (28) Dou, S.; Colby, R. H. Solution Rheology of a Strongly Charged Polyelectrolyte in Good Solvent. *Macromolecules* **2008**, *41*, 6505–6510, DOI: 10.1021/ma8001438.
- (29) Xu, F.; Zheng, S.-Z.; Luo, Y.-L.; Chen, T.-T. Synthesis, characterization, and micellization of pH-responsive poly(4-vinylpyridine)-block-poly(methacrylic acid) four-armed star-shaped block copolymers. *Macromolecular Research* **2013**, *21*, 977–986, DOI: 10.1007/s13233-013-1112-8.
- (30) Poggi, E.; Guerlain, C.; Debuigne, A.; Detrembleur, C.; Gigmes, D.; Hoeppener, S.; Schubert, U. S.; Fustin, C.-A.; Gohy, J.-F. Stimuli-responsive behavior of micelles prepared from a poly(vinyl alcohol)-block-poly(acrylic acid)-block-poly(4-vinylpyridine) triblock terpolymer. *European Polymer Journal* **2015**, *62*, 418–425, DOI: 10.1016/j.eurpolymj.2014.06.026.
- (31) Mauser, T.; Déjugnat, C.; Sukhorukov, G. B. Balance of Hydrophobic and Electrostatic Forces in the pH Response of Weak Polyelectrolyte Capsules. *The Journal of Physical Chemistry B* **2006**, *110*, 20246–20253, DOI: 10.1021/jp063502t.
- (32) Chen, Y.; Shull, K. R. High-Toughness Polycation Cross-Linked Triblock Copolymer Hydrogels. *Macromolecules* **2017**, *50*, 3637–3646, DOI: 10.1021/acs.macromol.7b00304.
- (33) Luzar, A.; Chandler, D. Structure and hydrogen bond dynamics of water-dimethyl sulfoxide mix-

- tures by computer simulations. *The Journal of Chemical Physics* **1993**, 98, 8160–8173, DOI: 10.1063/1.464521.
- (34) Trull, F. R.; Boiadjiev, S.; Lightner, D. A.; McDonagh, A. F. Aqueous dissociation constants of bile pigments and sparingly soluble carboxylic acids by 13C NMR in aqueous dimethyl sulfoxide: effects of hydrogen bonding. *J. Lipid Res.* **1997**, *38*, 1178–1188.
- (35) Mrázková, E.; Hobza, P. Hydration of Sulfo and Methyl Groups in Dimethyl Sulfoxide Is Accompanied by the Formation of Red-Shifted Hydrogen Bonds and Improper Blue-Shifted Hydrogen Bonds: An ab Initio Quantum Chemical Study. *J. Phys. Chem. A* **2003**, *107*, 1032–1039, DOI: 10.1021/jp026895e.
- (36) Vergenz, R. A.; Yazji, I.; Whittington, C.; Daw, J.; Tran, K. T. Computational Evidence for Methyl-Donated Hydrogen Bonds and Hydrogen-Bond Networking in 1,2-Ethanediol-Dimethyl Sulfoxide. *J. Am. Chem. Soc.* **2003**, *125*, 12318–12327, DOI: 10.1021/ja036516a.
- (37) Noack, K.; Kiefer, J.; Leipertz, A. Concentration-Dependent Hydrogen-Bonding Effects on the Dimethyl Sulfoxide Vibrational Structure in the Presence of Water, Methanol, and Ethanol. *ChemPhysChem* **2010**, *11*, 630–637, DOI: 10.1002/cphc.200900691.
- (38) Chand, A.; Chowdhuri, S. Effects of dimethyl sulfoxide on the hydrogen bonding structure and dynamics of aqueous N-methylacetamide solution. *J Chem Sci* **2016**, *128*, 991–1001, DOI: 10.1007/s12039-016-1092-2.
- (39) Sadman, K.; Wang, Q.; Chen, Y.; Keshavarz, B.; Jiang, Z.; Shull, K. R. Influence of Hydrophobicity on Polyelectrolyte Complexation. *Macromolecules* **2017**, *50*, 9417–9426, DOI: 10.1021/acs.macromol.7b02031.
- (40) Jaishankar, A.; McKinley, G. H. Power-law rheology in the bulk and at the interface: quasi-properties and fractional constitutive equations. *Proceedings of the Royal Society A: Mathematical, Physical and Engineering Sciences* **2012**, *469*, 20120284–20120284, DOI: 10.1098/rspa.2012.0284.

- (41) Samp, M. A.; Iovanac, N. C.; Nolte, A. J. Sodium Alginate Toughening of Gelatin Hydrogels. *ACS Biomaterials Science & Engineering* **2017**, *3*, 3176–3182, DOI: 10.1021/acsbiomaterials.7b00321.
- (42) Tsuchida, E.; Abe, K. *Interactions between macromolecules in solution and intermacromolecular complexes*.; Springer Berlin Heidelberg, 1982; pp 1–119.
- (43) Ohno, H.; Nii, A.; Tsuchida, E. Solvent effect on the complex formation of poly (methacrylic acid) with proton-accepting polymers. *Macromolecular Chemistry and Physics* **1980**, *181*, 1227–1235.
- (44) Bekturov, E. A.; Bimendina, L. A. Speciality Polymers; Springer, 1981; pp 99–147.
- (45) Smallwood, I. M. *Handbook of organic solvent properties*; Arnold; Halsted Press: London: New York, 1996.
- (46) Chen, S.; Chang, X.; Sun, P.; Zhang, W. Versatile multicompartment nanoparticles constructed with two thermo-responsive, pH-responsive and hydrolytic diblock copolymers. *Polym. Chem.* **2017**, *8*, 5593–5602, DOI: 10.1039/C7PY01182B.
- (47) Rubinstein, M.; Semenov, A. N. Dynamics of Entangled Solutions of Associating Polymers. *Macro-molecules* **2001**, *34*, 1058–1068, DOI: 10.1021/ma0013049.
- (48) Zhao, T.; Zhang, J.; Guo, B.; Zhang, F.; Sha, F.; Xie, X.; Wei, X. Density, viscosity and spectroscopic studies of the binary system of ethylene glycol+dimethyl sulfoxide at T=(298.15 to 323.15) K. *Journal of Molecular Liquids* **2015**, 207, 315–322, DOI: 10.1016/j.mollig.2015.04.001.
- (49) Ding, X.; Zhang, G.; Zhao, B.; Wang, Y. Unexpected viscoelastic deformation of tight sand-stone: Insights and predictions from the fractional Maxwell model. *Scientific Reports* **2017**, 7, DOI: 10.1038/s41598-017-11618-x.
- (50) Di Lorenzo, S.; Di Paola, M.; La Mantia, F. P.; Pirrotta, A. Non-linear viscoelastic behavior of polymer melts interpreted by fractional viscoelastic model. *Meccanica* 2017, 52, 1843–1850, DOI: 10.1007/s11012-016-0526-8.

- (51) Van Gurp, M.; Palmen, J. Time-temperature superposition for polymeric blends. *Rheol. Bull* **1998**, 67, 5–8.
- (52) Yeh, C. J.; Dowland, M.; Schmidt, R. G.; Shull, K. R. Fracture and thermal aging of resin-filled silicone elastomers. *Journal of Polymer Science Part B: Polymer Physics* **2016**, *54*, 263–273, DOI: 10.1002/polb.23919.
- (53) Trinkle, S.; Friedrich, C. Van Gurp-Palmen-plot: a way to characterize polydispersity of linear polymers. *Rheologica Acta* **2001**, *40*, 322–328.

For Table of Contents Graphic use only

Title: Tuning the Viscoelasticity of Hydrogen-Bonded Polymeric Materials through Solvent Composition

Authors: Lele Mathis, Yaoyao Chen, and Kenneth R. Shull

Email: k-shull@northwestern.edu

